Adsorption of Pb(II) from an Aqueous Solution by Titanium Dioxide/Carbon Nanotube Nanocomposites: Kinetics, Thermodynamics, and Isotherms†

Xiaowei Zhao, Qiong Jia,* Naizhong Song, Weihong Zhou, and Yusheng Li

College of Chemistry, Jilin University, Renmin Street #5988, Changchun 130022, P. R. China

In the present study, titanium dioxide/multiwalled carbon nanotubes (TiO_2/MWCNTs) nanocomposites have been synthesized, characterized, and used for the adsorption of Pb(II) from aqueous solution. The pH effect, kinetics, adsorption isotherms, and thermodynamics are examined in batch experiments. The time dependence of Pb(II) adsorption onto TiO_2/MWCNTs and MWCNTs nanocomposites can be described by a pseudosecond-order kinetic model. The Langmuir isotherm model agrees well with the equilibrium experimental data. The maximum adsorption capacity of TiO_2/MWCNTs and MWCNTs nanocomposites has been found to be (137.0 and 33.0) $mg \cdot g^{-1}$, respectively. Various thermodynamic parameters such as the Gibbs energy ($\Delta G°$), enthalpy ($\Delta H°$), and entropy ($\Delta S°$) changes are calculated. Our results have shown that TiO_2/MWCNTs nanocomposites can be used as an effective adsorbent for Pb(II) due to the high adsorption capacity as well as the short adsorption time needed to achieve equilibrium.

1. Introduction

In recent years, pollution of the environment by heavy metals has received considerable attention. Among all of the heavy metal ions, lead not only causes environmental pollution but also brings harm to people's health, and it has been identified as one of the most toxic heavy metals due to its detrimental effects on the human nervous system, blood circulation system, kidneys, and reproductive system. Nevertheless, direct determination of Pb(II) appears to be a difficult task because of insufficient sensitivity and matrix effects. Therefore, separation and preconcentration of trace metals prior to their analysis are often required. For this purpose, several methods have been developed, such as cloud point extraction,[1] coprecipitation,[2] and adsorption,[3] and so forth. Among all of the methods, adsorption has become increasingly popular because of its advantages of cost-effectiveness, simple operation, and environmental friendliness. Up to now, a variety of adsorbents have been reported as materials for the adsorption of heavy metals such as modified silica gel,[4−6] activated carbon,[7,8] biomaterials,[9−13] ion-imprinted materials,[14] inorganic materials,[15−18] polymers,[19] and sorption resins.[20] In spite of this, the search of new materials to develop novel adsorbents is of continuing interest.

Carbon nanotubes (CNTs) are increasingly attracting interest since their discovery.[21] Their small sizes, large surface area, high mechanical strength, and remarkable electrical conductivities give them potential for a wide range of promising applications.[22,23] Recently, CNTs have been found as the adsorbents for the removal of organic and inorganic contaminants.[24,25] Moreover, because of their relatively large specific area and hollow and layered structures, CNTs can also be used as support for adsorption materials.[26−29] Li et al.[30] have reported that CNT-supported amorphous Al_2O_3 has a higher fluoride adsorption capacity which is about 13.5 times higher than that of AC-300 carbon and 4 times higher than that of γ-Al_2O_3. Chen et al.[31] have found that iron oxide magnetic composites supported on CNTs can be used as effective adsorbents for the removal of Ni(II) and Sr(II) from wastewater. The adsorption capacity of the composites is much higher than that of MWCNTs and iron oxides. All of these facts show that the combination of CNTs with metal oxides can enhance adsorption capacity greatly. Except for the metal oxides mentioned above, titanium dioxide (TiO_2) has also been reported to possess a high adsorption capacity toward metal ions.[32−34] To enhance the adsorption capacity, some researchers have paid attention to the immobilization of TiO_2 on support materials, for example, silica gel.[6,35−37] For instance, Liang et al.[33] have investigated the adsorption behaviors of Cr(III) and Cr(VI) on immobilized nanometer TiO_2, indicating that the adsorption capacity for Cr(III) is 7.04 $mg \cdot g^{-1}$.

Because of the special structure of CNTs and the interaction between TiO_2 and CNTs,[30] it is of great interest to develop a new adsorbent combining TiO_2 with CNTs. The goal of this research was to immobilize TiO_2 on multiwalled carbon nanotubes (MWCNTs) and apply the synthesized TiO_2/MWCNTs to the sorption of Pb(II). The adsorption capacity of Pb(II) onto TiO_2/MWCNTs has been compared with that onto MWCNTs. The influence of experimental conditions, pH value, and contact time on the sorption behavior was investigated. The adsorption isotherm, kinetics, and thermodynamics have also been studied.

2. Experimental Section

2.1. Apparatus. The analysis was carried out using a flame atomic absorption spectrophotometer (FAAS) (Beijing Purkinje General Instruments Co., Ltd., China, http://www.pgeneral.com) equipped with a flame burner. Operational parameters for the metals under study, including lamp currents and wavelength, were those recommended by the manufacturer. All metals were measured under optimized operating conditions by FAAS with an air−acetylene flame.

† Part of the "Sir John S. Rowlinson Festschrift".

* Corresponding author. Telephone: +86 431 85095621. E-mail: jiaqiong@jlu.edu.cn.

10.1021/je100586r
Published on Web 09/29/2010

The oxidized MWCNTs and prepared TiO_2/MWCNTs nanocomposites were characterized using a transmission electron microscope (TEM) (JEM-2100F) with an accelerating voltage of 120 kV.

A pHS-3C digital pH meter (Rex Instruments Factory, Shanghai, China) was employed for the pH measurements. Deionized water was prepared by a Milli-Q SP system (Millipore, Milford, MA, USA).

2.2. Standard Solution and Reagents. MWNTs with a purity greater than 95 % were purchased from the Shenzhen Nanotech Port Co., Ltd. (China) with (10 to 30) nm diameters and (40 to 300) $m^2 \cdot g^{-1}$ in surface area. Titanium isopropoxide was supplied by the Shanghai Darui Chemical Reagent Co. Inc. (China) and used without further purification.

All chemicals used in this study were of analytical grade. Stock solutions (1000 $\mu g \cdot mL^{-1}$) of Pb were prepared by dissolving the appropriate amounts of $PbCl_2$ in deionized water. The working standard solutions were prepared daily by stepwise dilution of stock solutions. Adjustment of pH was undertaken using 0.1 $mol \cdot L^{-1}$ HCl and 0.1 $mol \cdot L^{-1}$ $NH_3 \cdot H_2O$. Deionized water was used through the work.

All containers were treated with 10 % (v/v) HNO_3 for at least 24 h, rinsed with high purity deionized water, and dried at room temperature before usage.

2.3. Synthesis of TiO_2/MWCNTs Nanocomposite. First, MWCNTs were purified as follows:[35] The MWCNTs were mixed with the acid mixture of concentrated sulfuric acid and nitric acid with a volume ratio of 3:1. The mixture was then heated to 140 °C (the boiling point of the mixture) for 20 min under refluxing and cooled naturally to room temperature. The layer deposited on the filter was washed with deionized water until the pH value reached neutrality. The product was then dried at 60 °C in an oven and kept in a desiccator for further use.

TiO_2/MWCNTs nanocomposites were synthesized following the surfactant wrapping sol−gel method.[38] Acid-treated MWCNTs were initially mixed with 0.5 % (by weight) sodium dodecylbenzenesulfonate in aqueous solution. The suspension was then treated by sonication overnight to obtain a stable solution with a high weight fraction of MWCNTs. The prepared MWCNTs solution was then dispersed in ethanol by stirring and mixed for 30 min to reach a uniform suspension (Solution I). A predetermined amount of titanium isopropoxide was mixed with ethanol and glacial acetic acid under stirring, which was kept for 30 min to form a clear solution (Solution II). Solution II was then added dropwise into Solution I under vigorous stirring, and the mixture was left at room temperature under stirring for 2 h to complete the reaction. Afterward, a diluted ammonia solution was added dropwise to hydrolyze the residual precursor (pH 9), leading to a uniform TiO_2 coating on the MWCNTs surface. Then, an amount of ethanol (MWCNTs:ethanol = 0.035:1, m/V) was added into the reaction system, and stirring was maintained for another 30 min. The suspension was centrifuged and washed with ethanol by three consecutive cycles. The final precipitate was dried in an oven at 60 °C for 10 h to obtain a powder product.

2.4. Batch Adsorption Studies. A portion of 0.02 g of adsorbent mixed with a 10 mL solution of Pb(II) in special glass-stoppered tubes were shaken under a controlled temperature of (293 ± 1) K unless otherwise stated. Batch adsorption experiments were conducted to investigate Pb(II) adsorption at various pH (2.0 to 7.0) and contact times [(10 to 210) min]. After reaching the sorption equilibrium, the suspension was filtered through 0.45 μm filters, and the metal concentration was determined in the liquid phase using FAAS.

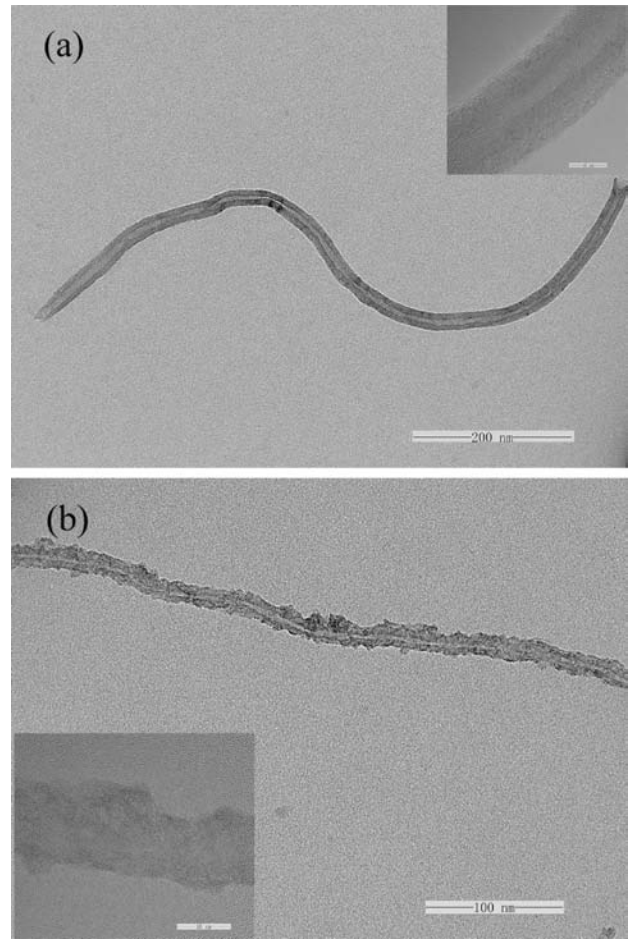

Figure 1. TEM images of oxidized MWCNTs (a) and TiO_2/MWCNTs composite (b). Inset: the magnified TEM images.

The adsorption capacity of the composites for Pb(II) was calculated according to the following equation:

$$q_e = \frac{(C_0 - C_e)V}{m} \quad (1)$$

where C_0 and C_e represent the initial and equilibrium metal ion concentrations ($mg \cdot L^{-1}$), respectively; V is the volume of the metal ion solution (mL), and m is the amount of adsorbent (mg).

3. Results and Discussion

3.1. TEM Observations. As is well-known, as-synthesized MWCNTs contain impurities such as catalyst particles, amorphous carbon, and fullerenes. After oxidation, the tips of MWCNTs may be opened, and fracturing takes place at positions where defects such as pentagons and heptagons exist. The morphology of the oxidized MWCNTs is shown in Figure 1a, showing that the oxidized MWCNTs are about 30 nm in diameter and several micrometers in length with a smooth and clean surface. This confirms that the oxidized MWCNTs are free of metal catalysts. Figure 1b shows the morphology of the prepared TiO_2/MWCNTs nanocomposites. The nanosize TiO_2 particles can be observed to be supported on the surfaces of the acid-treated MWCNTs. The goal of MWCNTs modification with TiO_2 has been achieved.

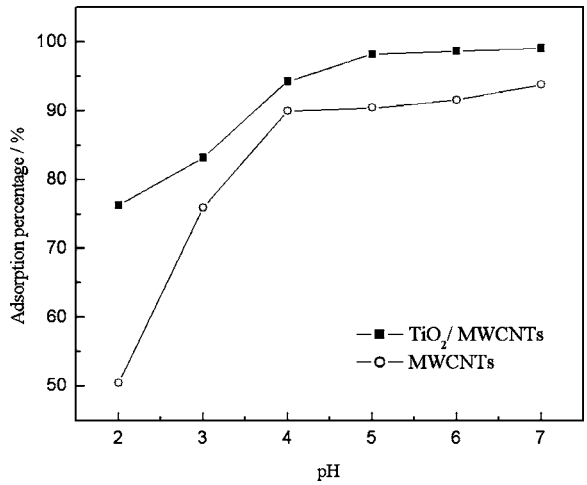

Figure 2. Effect of solution pH on the adsorption of Pb(II) onto TiO_2/MWCNTs and MWCNTs (dosage of adsorbent: 0.02 g, concentration of Pb: 10 mg·L^{-1}, contact time: 60 min).

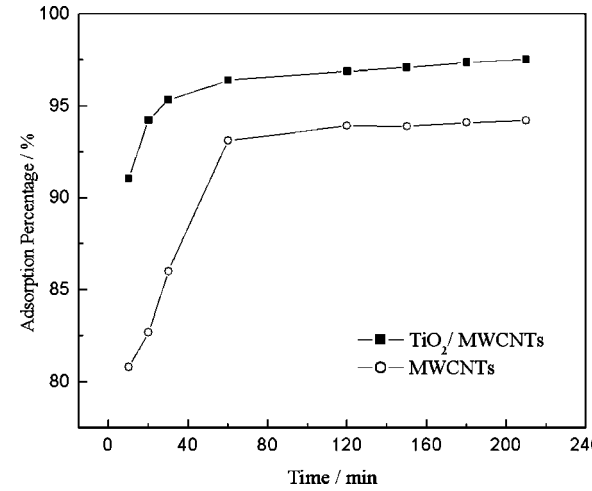

Figure 3. Effect of contact time on the adsorption of Pb(II) onto TiO_2/MWCNTs and MWCNTs (dosage of adsorbent: 0.02 g, concentration of Pb: 10 mg·L^{-1}, pH 6.0).

3.2. Effects of pH. Solution pH is one of the most important parameters affecting the adsorption process. In this study, the adsorption experiments have been conducted in the initial pH range of 2.0 to 7.0, and the results are presented in Figure 2. As a comparison, the adsorption performances of Pb(II) onto MWCNTs have also been shown. It is obvious that, at any pH value, the adsorption percentage of Pb(II) onto TiO_2/MWCNTs is higher than that onto MWCNTs. It can be concluded that the adsorption capacity can be enhanced when TiO_2 is immobilized onto MWCNTs. With increasing pH values, the adsorption percentage first increases and then changes negligibly. This phenomenon can be explained by the fact that the competition between protons and metal ions for the adsorption sites of the sorbent increases at lower pH values. To ensure quantitative adsorption and avoid precipitation at higher pH values, a sample pH of 6.0 was chosen as the optimum pH for further studies.

3.3. Adsorption Kinetics. Adsorption kinetics is investigated for a better understanding of the dynamics of adsorption. The effect of contact time on the adsorption of Pb(II) onto TiO_2/MWCNTs and MWCNTs is shown in Figure 3. It can be seen that the adsorption percentage of Pb(II) increases considerably until the contact time reaches 60 min. A further increase in contact time does not enhance the adsorption percentage obviously. A contact time of 60 min is selected for all of the equilibrium tests.

To investigate the adsorption kinetics of Pb(II) with the adsorbents, two kinetic models (pseudofirst-order and pseudo-second-order) were employed to simulate the experimental data.

The equation for pseudofirst-order kinetics is presented as follows:

$$\log(q_e - q_t) = \log q_e - \frac{k_1}{2.303}t \qquad (2)$$

where q_t and q_e are the amounts of Pb(II) adsorbed at time t and at equilibrium (mg·g^{-1}), respectively, and k_1 is the rate constant of the pseudofirst-order adsorption process (min^{-1}). The values of k_1 and q_e are calculated from the slope and intercept of plots of log ($q_e - q_t$) versus t (Figure 4).

The pseudosecond-order kinetic model can be expressed as:

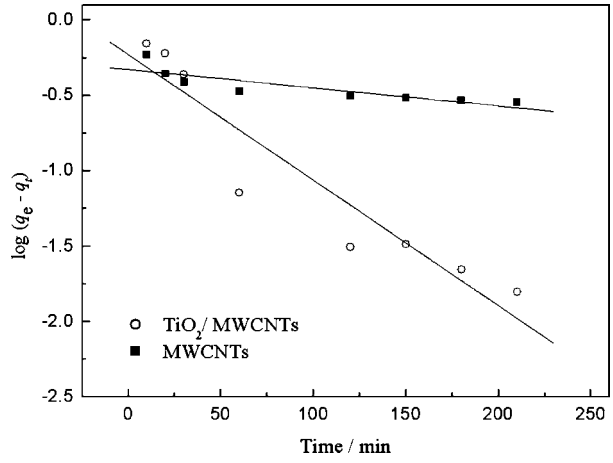

Figure 4. Pseudofirst-order kinetics plots for the adsorption of Pb(II) onto TiO_2/MWCNTs and MWCNTs.

$$\frac{t}{q_t} = \frac{1}{k_2 q_e^{\,2}} + \frac{1}{q_e}t \qquad (3)$$

where k_2 is the rate constant of the pseudosecond-order sorption (g·mg^{-1}·min^{-1}) which can be obtained by a plot of t/q_t against t (Figure 5).

The comparison (Table 1) made between the experimental adsorption capacity (q_{exp}) values and the calculated adsorption capacity (q_{cal}) values shows that q_{cal} values are very close to q_{exp} values for the pseudosecond-order kinetics. However, the q_{cal} values obtained from the pseudofirst-order kinetics model are different from the q_{exp} values. Moreover, the correlation coefficient values for pseudosecond-order model are much higher than that of pseudofirst-order model, suggesting that the adsorbent systems can be well-described by the pseudosecond-order kinetic model.

3.4. Adsorption Isotherms. In addition to adsorption kinetics, isotherm studies are undertaken to simulate the metal uptake by adsorbents. The Langmuir and the Freundlich isotherms are the most frequently used models to represent the equilibrium data of adsorption from aqueous solution.

The Langmuir isotherm assumes monolayer coverage of the adsorption surface and no subsequent interaction among ad-

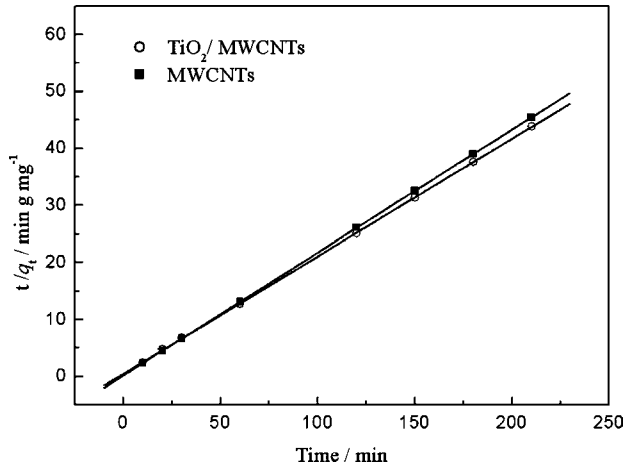

Figure 5. Pseudosecond-order kinetics plots for the adsorption of Pb(II) onto TiO_2/MWCNTs and/MWCNTs.

sorbed molecules. Therefore, the adsorption saturates, and no further adsorption can occur. The expression for the Langmuir isotherm is:

$$\frac{C_e}{q_e} = \frac{1}{q_{max}b} + \frac{C_e}{q_{max}} \quad (4)$$

where q_e and C_e are the adsorption capacity ($mg \cdot g^{-1}$) and the equilibrium concentration of the adsorbate ($mg \cdot L^{-1}$), respectively, while q_{max} and b represent the maximum adsorption capacity of adsorbents ($mg \cdot g^{-1}$) and the Langmuir adsorption constant ($L \cdot mg^{-1}$). The values of q_{max} and b are calculated from the slope and intercept of the linear plot of C_e/q_e against C_e.

The Freundlich isotherm was derived to model multilayer adsorption and adsorption on heterogeneous surfaces. It can be described as:

$$\log(q_e) = \frac{1}{n}\log(C_e) + \log K \quad (5)$$

where K and n are the Freundlich constants, which represent the adsorption capacity and the adsorption strength, respectively. K and n can be obtained from the intercept and the slope of the linear plot of $\log(q_e)$ versus $\log(C_e)$.

From Table 2, higher coefficients of determination indicate that the Langmuir model fits the adsorption data better than the Freundlich model. The maximum adsorption capacity q_{max} has also been calculated from the Langmuir equation, indicating that q_{max} of Pb(II) with TiO_2/MWCNTs and MWCNT are (137.0 and 33.0) $mg \cdot g^{-1}$, respectively. The q_{max} of Pb(II) with TiO_2/MWCNTs is much higher than that with MWCNT, which illustrates that the adsorption capacity of Pb(II) can be enhanced when TiO_2 is immobilized onto MWCNTs.

Table 2. Parameters of the Langmuir and Freundlich Isotherm for Pb(II) Adsorption

	Langmuir			Freundlich		
model	q_{max}/mg·g^{-1}	b/L·mg^{-1}	R^2	n	k	R^2
TiO_2/MWCNTs	137.0	0.03	0.9909	1.42	4.20	0.9667
MWCNTs	33.0	2.03	0.9978	2.11	3.73	0.9258

Table 3. Comparison of Adsorption of Pb(II) with Other Absorbents

adsorbent	pH	adsorption capacity/mg·g^{-1}	ref
nanometer titanium dioxide immobilized on silica gel	5.0	3.16	6
2-((2-aminoethylamino)methyl)phenol-functionalized activated carbon	4.0	16.20	8
seed husk of *Calophyllum inophyllum*	4.0	34.51	11
modified Duolite XAD-761 resins	4.0−7.0	46.66	20
oxidized MWCNTs	7.0−10.0	2.06	25
manganese oxide-coated CNTs	7.0	78.74	26
TiO_2/MWCNTs	6.0	137.00	this work

Table 4. Thermodynamic Parameters for Pb(II) Adsorption at 293 K

	$\Delta G°$	$\Delta H°$	$\Delta S°$
adsorbent	J·mol^{-1}	J·mol^{-1}	J·mol^{-1}·K^{-1}
TiO_2/MWCNTs	−2318.03	16926.5	65.681
MWCNTs	−1962.06	29637.7	107.849

The adsorption capacity of Pb(II) with TiO_2/MWCNT has also been compared with other absorbents. Results are shown in Table 3. It can be seen that TiO_2/MWCNTs is a fairly good Pb(II) absorber with quite a high adsorption capacity.

3.5. Adsorption Thermodynamics. The thermodynamic parameters provide in-depth information on inherent energetic changes that are associated with adsorption; therefore, they should be properly evaluated. The Gibbs energy ($\Delta G°$), enthalpy ($\Delta H°$), and entropy ($\Delta S°$) changes are calculated in this study to predict the process of adsorption. The distribution coefficient (K_d) is calculated according to the following equation:

$$K_d = \frac{q_e}{C_e} \quad (6)$$

The values of enthalpy ($\Delta H°$) and entropy ($\Delta S°$) are calculated from the slopes and intercepts of a plot of ln K_d versus $1/T$ by using the equation:

$$\ln K_d = \frac{\Delta S°}{R} - \frac{\Delta H°}{RT} \quad (7)$$

The Gibbs energy ($\Delta G°$) of adsorption is calculated from the equation:

$$\Delta G° = \Delta H° - T\Delta S° \quad (8)$$

Table 1. Kinetic Parameters for the Adsorption of Pb(II) onto TiO_2/MWCNTs and MWCNTs

	pseudofirst-order model				pseudosecond-order model		
adsorbent	$q_{e,exp}$ / mg·g^{-1}	k_1 / g·mg^{-1}·min^{-1}	$q_{e,cal}$ / mg·g^{-1}	R^2	k_2 / g·mg^{-1}·min^{-1}	$q_{e,cal}$ / mg·g^{-1}	R^2
TiO_2/MWCNTs	4.91	0.0028	0.47	0.7340	0.26	4.63	1.0
MWCNTs	4.81	0.02	0.59	0.8918	0.09	4.86	0.9999

where R (8.3145 $J \cdot mol^{-1} \cdot K^{-1}$) is the ideal gas constant and T (K) is the absolute temperature. The calculated values of thermodynamic parameters are listed in Table 4. The positive values of $\Delta H°$ for Pb(II) (Table 3) suggest an endothermic nature of adsorption. The negative values of $\Delta G°$ indicate the spontaneous nature of the reaction, while the positive values for $\Delta S°$ reflect an increase in the randomness at the solid−solution interface during the adsorption process. The thermodynamic parameters are actually helpful in the practical application of the process.

4. Conclusions

In this work, TiO_2/MWCNTs nanocomposites have been successfully prepared and used to remove Pb(II) ion from aqueous solution. The pH effect, kinetics, adsorption isotherms, and thermodynamics were examined in batch experiments. The adsorption kinetics follows the pseudosecond-order rate model very well. The equilibrium data have been well-described by the Langmuir isotherm. Thermodynamic parameters suggest that the adsorption process is spontaneous and endothermic in nature. The maximum adsorption capacity of TiO_2/MWCNTs nanocomposites for Pb(II) has been determined as 137.0 $mg \cdot g^{-1}$, which is much higher than that with MWCNTs (33.0 $mg \cdot g^{-1}$). Because of its high adsorption capacity and short adsorption time to achieve equilibrium, this type of TiO_2/MWCNTs nanocomposite can be used as a potential sorbent in the field of preconcentration procedures.

Literature Cited

(1) Ghaedi, M.; Shokrollahi, A.; Niknam, K.; Niknam, E.; Najibi, A.; Soylak, M. Cloud point extraction and flame atomic absorption spectrometric determination of cadmium(II), lead(II), palladium(II) and silver(I) in environmental samples. *J. Hazard. Mater.* **2009**, *168*, 1022–1027.

(2) Uluozlu, O. D.; Tuzen, M.; Mendil, D.; Soylak, M. Coprecipitation of trace elements with Ni^{2+}/2-Nitroso-1-naphthol-4-sulfonic acid and their determination by flame atomic absorption spectrometry. *J. Hazard. Mater.* **2010**, *176*, 1032–1037.

(3) Pehlivan, E.; Altun, T. Ion-exchange of Pb^{2+}, Cu^{2+}, Zn^{2+}, Cd^{2+}, and Ni^{2+} ions from aqueous solution by Lewatit CNP 80. *J. Hazard. Mater.* **2007**, *140*, 299–307.

(4) Thu, P. T. T.; Thanh, T. T.; Phi, H. N.; Kim, S. J.; Vo, V. Adsorption of lead from water by thiol-functionalized SBA-15 silicas. *J. Mater. Sci.* **2010**, *45*, 2952–2957.

(5) Yin, P.; Xu, Q.; Qu, R.; Zhao, G.; Sun, Y. Adsorption of transition metal ions from aqueous solutions onto a novel silica gel matrix inorganic-organic composite material. *J. Hazard. Mater.* **2010**, *173*, 710–716.

(6) Liu, R.; Liang, P. Determination of trace lead in water samples by graphite furnace atomic absorption spectrometry after preconcentration with nanometer titanium dioxide immobilized on silica gel. *J. Hazard. Mater.* **2008**, *152*, 166–171.

(7) Lalhruaitluanga, H.; Jayaram, K.; Prasad, M. N. V.; Kumar, K. K. Lead(II) adsorption from aqueous solutions by raw and activated charcoals of Melocanna baccifera Roxburgh (bamboo)-A comparative study. *J. Hazard. Mater.* **2010**, *175*, 311–318.

(8) He, Q.; Hu, Z.; Jiang, Y.; Chang, X.; Tu, Z.; Zhang, L. Preconcentration of Cu(II), Fe(III) and Pb(II) with 2-((2-aminoethylamino) -methyl)phenol-functionalized activated carbon followed by ICP-OES determination. *J. Hazard. Mater.* **2010**, *175*, 710–714.

(9) Zhang, J. P.; Wang, A. Q. Adsorption of Pb(II) from aqueous solution by chitosan-g-poly(acrylic acid)/attapulgite/sodium humate composite hydrogels. *J. Chem. Eng. Data* **2010**, *55* (7), 2379–2384.

(10) Munagapati, V. S.; Yarramuthi, V.; Nadavala, S. K.; Alla, S. R.; Abburi, K. Biosorption of Cu(II), Cd(II) and Pb(II) by acacia leucocephala bark powder: kinetics, equilibrium and thermodynamics. *Chem. Eng. J.* **2010**, *157*, 357–365.

(11) Lawal, O. S.; Sanni, A. R.; Ajayi, I. A.; Rabiu, O. O. Equilibrium, thermodynamic and kinetic studies for the biosorption of aqueous lead(II) ions onto the seed husk of *Calophyllum inophyllum*. *J. Hazard. Mater.* **2010**, *177*, 829–835.

(12) Chakravarty, S.; Mohanty, A.; Sudha, T. N.; Upadhyay, A. K.; Konar, J.; Sircar, J. K.; Madhukar, A.; Gupta, K. K. Removal of Pb(II) ions from aqueous solution by adsorption using bael leaves (*Aegle marmelos*). *J. Hazard. Mater.* **2010**, *173*, 502–509.

(13) Kamal, M. H. M. A.; Azira, W. M. K. W. K.; Kasmawati, M.; Haslizaidi, Z.; Saime, W. N. W. Sequestration of toxic Pb(II) ions by chemically treated rubber (*Hevea brasiliensis*) leaf powder. *J. Environ. Sci.* **2010**, *22*, 248–256.

(14) Pan, J. Y.; Wang, S.; Zhang, R. F. A novel Pb(II)-imprinted IPN for selective preconcentration of lead from water and sediments. *Int. J. Environ. Anal. Chem.* **2006**, *86*, 855–865.

(15) Jiang, M. Q.; Jin, X. Y.; Lu, X. Q.; Chen, Z. L. Adsorption of Pb(II), Cd(II), Ni(II) and Cu(II) onto natural kaolinite clay. *Desalination* **2010**, *252*, 33–39.

(16) Chen, S. B.; Ma, Y. B.; Chen, L.; Wang, L. Q.; Guo, H. T. Comparison of Pb(II) immobilized by bone char meal and phosphate rock: characterization and kinetic study. *Arch. Environ. Contam. Toxicol.* **2010**, *58*, 24–32.

(17) Eloussaief, M.; Benzina, M. Efficiency of natural and acid-activated clays in the removal of Pb(II) from aqueous solutions. *J. Hazard. Mater.* **2010**, *178*, 753–757.

(18) Mahmoud, M. E.; Osman, M. M.; Hafez, O. F.; Elmelegy, E. Removal and preconcentration of lead (II), copper (II), chromium (III) and iron (III) from wastewaters by surface developed alumina adsorbents with immobilized 1-nitroso-2-naphthol. *J. Hazard. Mater.* **2010**, *173*, 349–357.

(19) Liu, J.; Ma, Y.; Xu, T.; Shao, G. Preparation of zwitterionic hybrid polymer and its application for the removal of heavy metal ions from water. *J. Hazard. Mater.* **2010**, *178*, 1021–1029.

(20) Tharanitharan, V.; Srinivasan, K. Kinetic and equilibrium studies of removal of Pb(II) and Cd(II) ions from aqueous solution by modified duolite XAD-761 resins. *Asian J. Chem.* **2010**, *22*, 3036–3046.

(21) Iijima, S. Helical microtubules of graphitic carbon. *Nature* **1991**, *354*, 56–58.

(22) Dai, H.; Hafner, J. H.; Rinzler, A. G.; Colbert, D. T.; Smalley, R. E. Nanotubes as nanoprobes in scanning probe microscopy. *Nature* **1996**, *384*, 147–150.

(23) Kong, J.; Franklin, N. R.; Zhou, C.; Chapline, M. G.; Peng, S.; Cho, K.; Dai, H. Nanotube molecular wires as chemical sensors. *Science* **2000**, *287*, 622–625.

(24) Valcarcel, M.; Cardenas, S.; Simonet, B. M.; Moliner-Martinez, Y.; Lucena, R. Carbon nanostructures as sorbent materials in analytical processes. *TrAC, Trends Anal. Chem.* **2008**, *27*, 34–43.

(25) Xu, D.; Tan, X.; Chen, C.; Wang, X. Removal of Pb(II) from aqueous solution by oxidized multiwalled carbon nanotubes. *J. Hazard. Mater.* **2008**, *154*, 407–416.

(26) Wang, S. G.; Gong, W. X.; Liu, X. W.; Yao, Y. W.; Gao, B. Y.; Yue, Q. Y. Removal of lead(II) from aqueous solution by adsorption onto manganese oxide-coated carbon nanotubes. *Sep. Purif. Technol.* **2007**, *58*, 17–23.

(27) Peng, X.; Luan, Z.; Di, Z.; Zhang, Z.; Zhu, C. Carbon nanotubes-iron oxides magnetic composites as adsorbent for removal of Pb(II) and Cu(II) from water. *Carbon* **2005**, *43*, 855–894.

(28) Amais, R. S.; Ribeiro, J. S.; Segatelli, M. G.; Yoshida, I. V. P.; Luccas, P. O.; Tarley, C. R. T. Assessment of nanocomposite alumina supported on multi-wall carbon nanotubes as sorbent for on-line nickel preconcentration in water samples. *Sep. Purif. Technol.* **2007**, *58*, 122–128.

(29) Di, Z. C.; Ding, J.; Peng, X. J.; Li, Y. H.; Luan, Z. K.; Liang, J. Chromium adsorption by aligned carbon nanotubes supported ceria nanoparticles. *Chemosphere* **2006**, *62*, 861–865.

(30) Li, Y. H.; Wang, S.; Cao, A.; Zhao, D.; Zhang, X.; Xu, C.; Luan, Z.; Ruan, D.; Liang, J.; Wu, D.; Wei, B. Adsorption of fluoride from water by amorphous alumina supported on carbon nanotubes. *Chem. Phys. Lett.* **2001**, *350*, 412–416.

(31) Chen, C.; Hu, J.; Shao, D.; Li, J.; Wang, X. Adsorption behavior of multiwall carbon nanotube/iron oxide magnetic composites for Ni(II) and Sr(II). *J. Hazard. Mater.* **2009**, *164*, 923–928.

(32) Huang, C. Z.; Jiang, Z. C.; Hu, B. Mesoporous titanium dioxide as a novel solid-phase extraction material for flow injection micro-column preconcentration on-line coupled with ICP-OES determination of trace metals in environmental samples. *Talanta* **2007**, *73*, 274–281.

(33) Liang, P.; Qin, Y. C.; Hu, B.; Peng, T. Y.; Jiang, Z. C. Nanometer-size titanium dioxide microcolumn on-line preconcentration of trace metals and their determination by inductively coupled plasma atomic emission spectrometry in water. *Anal. Chim. Acta* **2001**, *440*, 207–213.

(34) Li, S.; Deng, N. Separation and preconcentration of Se(IV)/Se(VI) species by selective adsorption onto nanometer-sized titanium dioxide and determination by graphite furnace atomic absorption spectrometr. *Anal. Bioanal. Chem.* **2002**, *374*, 1341–1345.

(35) Liu, Y.; Liang, P.; Guo, L. Nanometer titanium dioxide immobilized on silica gel as sorbent for preconcentration of metal ions prior to their determination by inductively coupled plasma atomic emission spectrometry. *Talanta* **2005**, *68*, 25–30.

(36) Liang, P.; Cao, J.; Liu, R.; Liu, Y. Determination of trace rare earth elements by inductively coupled plasma optical emission spectrometry after preconcentration with immobilized nanometer titanium dioxide. *Microchim. Acta* **2007**, *159*, 35–40.
(37) Liang, P.; Ding, Q.; Liu, Y. Speciation of chromium by selective separation and preconcentration of Cr(III) on an immobilized nanometer titanium dioxide microcolumn. *J. Sep. Sci.* **2006**, *29*, 242–247.
(38) Gao, B. Y.; Chen, G. Z.; Puma, G. L. Carbon nanotubes/titanium dioxide ($CNTs/TiO_2$) nanocomposites prepared by conventional and novel surfactant wrapping sol-gel methods exhibiting enhanced photocatalytic activity. *Appl. Catal., B* **2009**, *89*, 503–509.

Received for review May 29, 2010. Accepted September 3, 2010. Financial support was provided by the Basic Scientific Research Fund of Jilin University (2008).

JE100586R